IEEE Access
Multidisciplinary | Rapid Review | Open Access Journal

Received November 14, 2020, accepted November 21, 2020, date of publication December 1, 2020,
date of current version December 10, 2020.

Digital Object Identifier 10.1109/ACCESS.2020.3041769

Maximum Efficiency Tracking for Dynamic WPT System Based on Optimal Input Voltage Matching

HAO HE, SONGCEN WANG, YOUWEI LIU, CHENG JIANG, XIAOKANG WU, BIN WEI, AND BINGWEI JIANG
China Electric Power Research Institute, Beijing 100192, China

Corresponding author: Hao He (hehao_cn@163.com)

This work was supported by the Science and Technology Project of State Grid Corporation of China Research on High Performance Wireless Power Transmission Technology Based on Silicon Carbide Power Devices under Grant DGB17201900333.

ABSTRACT Wireless power transfer (WPT) technology has drawn much attention due to its advantages such as safety, convenience, and non-contact. For some movable devices such as intelligent inspection robot, the constant output voltage is very important to ensure its normal operation. In order to improve the system efficiency and steadiness of output voltage, a maximum efficiency tracking and constant voltage charging method is proposed for the dynamic WPT system. In this method, the mutual inductance and optimal input voltage can be estimated accurately no matter the coupling coefficient and equivalent load change or not. The simulation and experimental results have shown that the WPT system realize maximum efficiency tracking and constant voltage charging when the resistance is changed from 10Ω to 5Ω, and the same result was achieved when the mutual inductance is altered from 20μH to 10μH.

INDEX TERMS Wireless power transfer, optimal input voltage matching, maximum efficiency tracking.

I. INTRODUCTION

Recently, wireless power transfer (WPT) technology has drawn much attention from the academic and industrial circles for its advantages such as safety, convenience, and non-contact [1]–[3]. It has been applied in electric vehicles (EVs), smart phone and many other low-power fields like implantable medical electronics, and domestic appliances [3]–[7]. In general, constant current (CC) charging is necessary for batteries and supercapacitors [8], [9]. However, as for some movable devices such as intelligent inspection robot (shown in Fig.1), the constant output voltage is the key to ensure its normal operation.

For a dynamic WPT system, the mutual inductance is unstable because of the variable position and distance of primary and secondary coils [8]. It is difficult for the system to maintain high efficiency during the whole moving process. Therefore, the ways to realize the maximum efficiency tracking (MET) on the dynamic WPT system and obtain the constant output voltage simultaneously is an important topic.

The associate editor coordinating the review of this manuscript and approving it for publication was Shihong Ding.

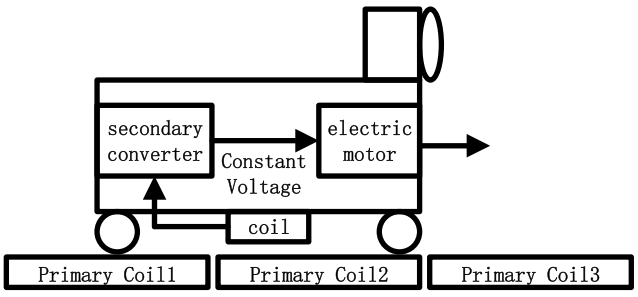

FIGURE 1. The sketch of the dynamic WPT system for intelligent inspection robot.

At present, many measures have been proposed to improve the efficiency of the WPT system, which can be mainly divided into the following two schemes:

1) Ensure the impedance of the resonant circuit matched when the distance of the coils changes. For a WPT system, the resonant frequency will change along with the variation of coupling coefficient. In [10] and [11], a novel series/parallel capacitance array and impedance matching circuit are used to regulate the resonant frequency of the resonant circuit to be equal to the working frequency. In [12], a multiloop topology is employed

to greatly reduce the variation of the input impedance of the WPT system. In [13], a novel MET control method of the WPT system is proposed with optimized T-type impedance matching network under the real-time identification of a coupling coefficient to realize the MET control. In [14], a real-time range-adaptive impedance matching utilizing a machine learning strategy is used for a tunable matching network to improving the efficiency. However, it is necessary for the impedance matching technology to adjust the parameters of resonant circuit when the system is running. It is more suitable for low-powered and high-frequency WPT system [16].

2) Adjust the equivalent load resistance to be equal to the optimal value. In [15]–[17], the secondary side achieves the constant current charging, and the primary side searches the minimum DC input current to realize the maximum efficiency tracking. However, this method cannot track the maximum efficiency when the coupling coefficient changes greatly like in the dynamic WPT system. In [18], a dynamic coupling coefficient estimation method is proposed to achieve the maximum efficiency tracking. The primary side realizes the constant current charging, and the secondary side realizes coupling coefficient estimation and optimal resistance matching. However, this method only verifies the MET in a static WPT system. And the delay of wireless communication will reduce the real-time performance of current control loop. It is not suitable for dynamic WPT system due to its poor dynamic performance. In [19] and [20], a discontinuous operation inverter is used to match the optimal input impedance of the system. This method reduces the weight and volume of the system greatly, but the ripple of output voltage is much larger than other methods.

In the previous studies, few papers consider the maximum efficiency tracking on dynamic WPT system. In fact, the equivalent load of the secondary side changes according to the running state such as the speed and weight of the movable device. Besides, the change of the position leads to drastic change of mutual inductance. These factors will cause lower efficiency of the dynamic WPT system.

This paper proposed a novel maximum efficiency tracking method for the dynamic WPT system. In this method, the mutual inductance and optimal input voltage can be estimated periodically. The control loops of the primary side and secondary side are independent. For the secondary side, a buck-boost converter is used to achieve accurate CV charging with a PI controller. For the primary side, the maximum efficiency tracking is realized by adjusting the input voltage of the inverter to be equal to the optimal value. Whether mutual inductance or equivalent load resistance changes or not, the MET and CV charging method can be realized.

The rest of the paper is organized as follows: In section II, the model of the WPT system with LCC-S topology is established, and the relationship between the efficiency and equivalent load as well as that between the efficiency and mutual inductance are analyzed. In section III, the mutual inductance estimation and optimal input voltage matching method are analyzed with mathematical derivation, and the control scheme is also given in the form of flow chart. In section IV, the MET and CV charging method based on the analysis in section III are experimentally verified. The differences between the proposed and previous methods are also discussed.

II. SYSTEM STRUCTURE AND CIRCUIT ANALYSIS

A. SYSTEM STRUCTURE

A WPT system is generally composed of primary side and secondary side divided by magnetic coupler, and different resonant circuits are designed for the two coils [16]–[18]. In previous studies, four basic resonant topologies, S-S, S-P, P-S, and P-P, have been widely adopted. But only the resonant frequency of S-S topology is independent of mutual inductance [21]. Recently, high-order resonant circuits such as LCL, LCC are also adopted. The LCC topology has the character that the current of primary coil is not affected by load and mutual inductance. It is more stable and secure than other topologies when there is large misalignment between primary and secondary coils [22]–[24]. The typical WPT system with LCC-S topology is shown in Fig.2.

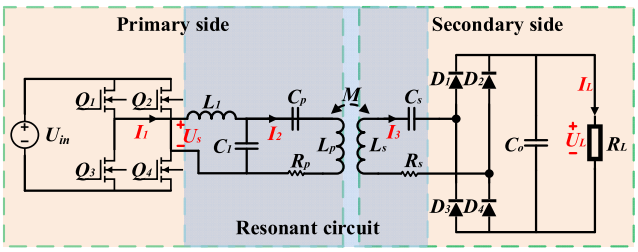

FIGURE 2. Structure of LCC/S compensated WPT system.

In Fig.2, U_{in}, U_s are the input and equivalent fundamental output voltage of inverter which is composed of SiC MOSFETs $Q_1 \sim Q_4$. An H-bridge rectifier consisted of four SiC diodes $D_1 \sim D_4$ is adopted at the secondary side. C_o is the smoothing capacitor. L_p, C_p and L_s, C_s, constitute the resonant network of primary and secondary sides, respectively. R_p and R_s are the internal resistances of L_p and L_s, respectively. L_1 and C_1 are series inductor and parallel resonant capacitor of the LCC topology. M is the mutual inductance between the primary and secondary coils. It should be noted that since the internal resistance of L_1 is far less than that of the coils, it can be ignored to simplify the progress of system analysis [16], [25].

B. CIRCUIT AND EFFICIENCY ANALYSIS

The equivalent circuit model of the LCC-S topology is shown in Fig.3. The input voltage U_s is a sinusoidal alternating

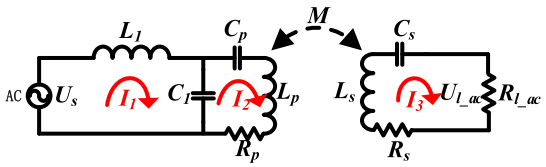

FIGURE 3. Equivalent circuit model.

voltage source whose frequency is equal to the resonant frequency of the resonant circuit.

According to Kirchhoff's voltage law (KVL), the following equations based on fundamental harmonic analysis (FHA) are deduced as [10], [25]:

$$\begin{cases} \dot{U}_s = \left(j\omega L_1 + \dfrac{1}{j\omega C_1}\right)\dot{I}_1 - \dfrac{1}{j\omega C_1}\dot{I}_2 \\ 0 = \left(\dfrac{1}{j\omega C_1} + \dfrac{1}{j\omega C_p} + j\omega L_p + R_p\right)\dot{I}_2 - \dfrac{1}{j\omega C_1}\dot{I}_1 - j\omega M\dot{I}_3 \\ 0 = \left(\dfrac{1}{j\omega C_s} + j\omega L_s + R_s + R_l\right)\dot{I}_3 - j\omega M\dot{I}_2 \end{cases} \quad (1)$$

where $\dot{U}_s$ and $\dot{I}_1$ are phasors of input voltage and current of LCC topology. $\dot{I}_2$ and $\dot{I}_3$ are the current of the primary and secondary coils, respectively. ω is the angular frequency of system, and satisfies $\omega = 2\pi f$.

According to [16], [22]–[24], the parameters of the LCC-S topology are determined by the following principles:

$$\begin{cases} j\omega L_1 + \dfrac{1}{j\omega C_1} = 0 \\ \dfrac{1}{j\omega C_1} + \dfrac{1}{j\omega C_p} + j\omega L_p = 0 \\ \dfrac{1}{j\omega C_s} + j\omega L_s = 0 \end{cases} \quad (2)$$

According to (1) and (2), when the WPT system works in resonant state [10], [25], the output voltage $\dot{U}_l$ and power P_{out} can be expressed as:

$$\dot{U}_l = \frac{\dot{U}_s M R_l}{L_1 (R_l + R_s)} \quad (3)$$

$$P_{out} = \frac{U_s^2 M^2 R_l}{L_1^2 (R_l + R_s)^2} \quad (4)$$

It can be seen from (3) and (4) that the output voltage and power are function of M and R_l when the input voltage is constant. Besides, the input power P_{in} is given by:

$$P_{in} = \frac{U_S^2 R_p}{\omega^2 L_1^2} + \frac{U_s^2 M^2}{L_1^2 (R_l + R_s)} \quad (5)$$

Divide (4) by (5) [18], [25], the efficiency of the system can be derived as:

$$\eta = \frac{P_{out}}{P_{in}} = \frac{(\omega M)^2 R_l}{(R_l + R_S)\left[R_P (R_l + R_S) + (\omega M)^2\right]} \quad (6)$$

In a WPT system, R_p, R_s can be measured and ω are immutable. It is obvious that η is related to M and R_l. According to the data in Table 1, the efficiency versus the equivalent resistance under different values of the mutual inductance is plotted in Fig.4.

TABLE 1. System Parameters.

Symbol	Value	Symbol	Value
L_1	25.2μH	L_s	58.9μH
C_1	139.1nF	C_s	59.5nF
L_p	361.9μH	R_s	0.3Ω
C_p	10.4nF	f	85kHz
R_p	0.5Ω	R_l	5Ω/10Ω
M	8~22μH		

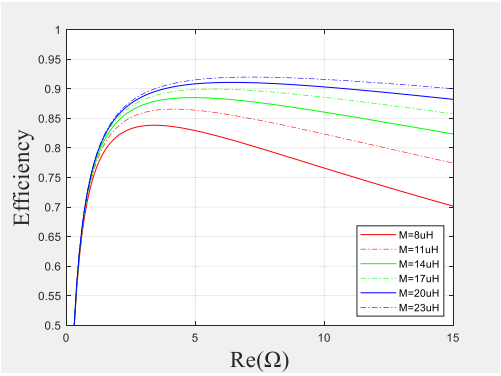

FIGURE 4. η versus R_l under different values of the mutual inductance.

It is shown in Fig.4 that there are different optimal equivalent resistance R_{l_opt} under the conditions of different mutual inductance. When the load resistance is equal to R_{l_opt}, the efficiency of the system reaches the highest level. Once R_l is not equal to R_{l_opt}, the efficiency will decrease rapidly. In conclusion, the essence of the MET control method is to adjust the load resistance to be equal to the optimal value.

By taking the derivative of (6) with respect to R_l [18], [20], the optimal equivalent resistance can be obtained as:

$$\begin{cases} \dfrac{d\eta}{dR_l} = 0 \\ \dfrac{d^2\eta}{dR_l^2} < 0 \end{cases} \rightarrow R_{l\_opt} = R_s\sqrt{1 + \frac{(\omega M)^2}{R_P R_s}} \quad (7)$$

It can be seen from (7) that R_{l_opt} is related to the mutual inductance while ω, R_p and R_s are constant. Once the mutual inductance is estimated, the optimal equivalent resistance can be calculated.

III. MET AND CV CHARGING METHOD FOR DYNAMIC WPT SYSTEM

A. CONSTANT OUTPUT VOLTAGE CONTROL

The main circuit diagram of the dynamic WPT system is shown in Fig.5. A buck converter and buck-boost converter are designed on primary and secondary side, respectively. It can be seen from (4) and (6) that the output voltage and the system efficiency are related to the mutual inductance and equivalent load resistance. However, the load resistance and

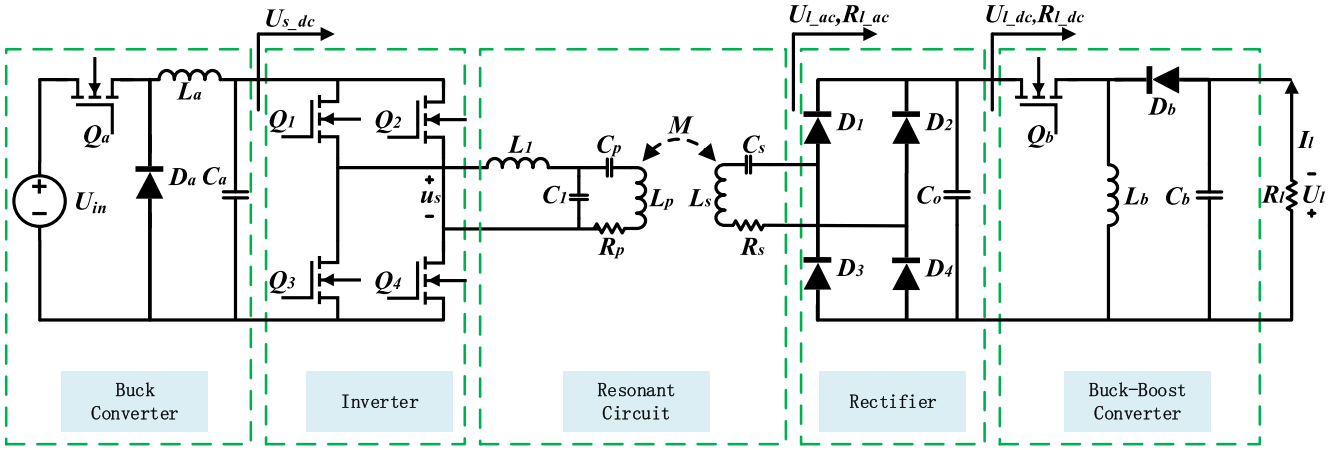

FIGURE 5. Main circuit diagram of WPT system.

mutual inductance is not constant when the device is moving. So, a buck-boost converter is designed on the secondary side to realize the constant voltage charging.

According to the principle of the buck-boost converter at continuous current mode (CCM), the relationship between input voltage U_{l_dc} and output voltage U_l is given by (8). The relationship between equivalent input resistance R_{l_dc} and load resistance R_l is given by (9).

$$U_{l\_dc} = \frac{U_l\,(1-d_2)}{d_2} \tag{8}$$

$$R_{l\_dc} = \left(\frac{1-d_2}{d_2}\right)^2 R_l \tag{9}$$

where d_2 is the duty cycle of buck-boost converter. It can be seen from (8) that $U_{l\_dc} > U_l$ when $d_2 < 0.5$, and $U_{l\_dc} < U_l$ when $d_2 > 0.5$. So, we can adjust d_2 to keep the output voltage constant no matter the input voltage is greater or less than the output voltage. In addition, a PI controller is adopted in the secondary side to reduce the ripple of output voltage. This will greatly improve the stability of the system.

B. MUTUAL INDUCTANCE ESTIMATE

As for the H-bridge rectifier, assuming there is no voltage drop, the relationship between U_{l_ac} and U_{l_dc} is given by (10), and the relationship between R_{l_ac} and R_{l_dc} is given by (11) [15], [16].

$$U_{l\_ac} = \frac{2\sqrt{2}}{\pi} U_{l\_dc} \tag{10}$$

$$R_{l\_ac} = \frac{8}{\pi^2} R_{l\_dc} \tag{11}$$

where U_{l_ac} and R_{l_ac} are equivalent input voltage and equivalent input resistance of the rectifier. And U_{l_dc} and R_{l_dc} is given in (8) and (9), then the U_{l_ac} and R_{l_ac} can be derived as:

$$U_{l\_ac} = \frac{2\sqrt{2}U_l\,(1-d_2)}{\pi d_2} \tag{12}$$

$$R_{l\_ac} = \frac{8}{\pi^2}\left(\frac{1-d_2}{d_2}\right)^2 R_l \tag{13}$$

According to (3), (12) and (13), the mutual inductance M can be derived as:

$$M = \left(\frac{2\sqrt{2}\,(1-d_2)}{\pi d_2} + \frac{\sqrt{2}\pi R_s d_2}{4R_l\,(1-d_2)}\right)\frac{U_l L_1}{U_s} \tag{14}$$

where U_s is equivalent fundamental output voltage of the H-bridge inverter. It can be given by:

$$U_s = \frac{2\sqrt{2}}{\pi} U_{s\_dc} \tag{15}$$

From (14), we can find that the mutual inductance M is a function of d_2, U_s and R_l. Other parameters are constant. Consequently, a wireless communication network is necessary to transfer the value of d_2 and R_l from secondary side to primary side.

C. OPTIMAL VOLTAGE MATCHING

When the system is working at the point of maximum efficiency, the equivalent input resistance can be calculated from (7), and the duty cycle of the buck-boost can be derived from (7), (9) and (11) as:

$$d_{2\_opt} = \frac{1}{1+\sqrt{\frac{\pi^2 R_{l\_opt}}{8R_l}}} \tag{16}$$

Due to R_l is constant, the optimal AC voltage of secondary side can be derived from (8), (11) and (16) as:

$$U_{l\_ac\_opt} = \frac{2\sqrt{2}}{\pi}\frac{U_l\left(1-d_{2\_opt}\right)}{d_{2\_opt}} = U_l\sqrt{\frac{R_{l\_opt}}{R_l}} \tag{17}$$

According to (3) and (17), the optimal equivalent output voltage of inverter can be given by (18):

$$U_{s\_opt} = \frac{L_1\,(R_l+R_s)\,U_{l\_ac\_opt}}{MR_l} \tag{18}$$

Substituting (14), (17) into (18), the optimal input voltage of the inverter can be derived as:

$$U_{s\_dc\_opt} = \frac{1}{\alpha+\beta}\frac{U_{s\_dc\_pre}\,(R_l + R_s)}{R_l}\sqrt{\frac{R_{l\_opt}}{R_l}} \tag{19}$$

where $\alpha = \frac{2\sqrt{2}(1-d_2)}{\pi d_2}$, $\beta = \frac{\sqrt{2}\pi R_s d_2}{4R_l(1-d_2)}$, and $U_{s\_dc\_pre}$ is previous input voltage of inverter which is used to estimate mutual inductance.

In (19), the system parameters other than mutual inductance are known, and the output voltage is stable when the system works at CV mode. Before estimating the optimal input voltage of inverter, the mutual inductance can also be estimated by (14). What should be done is adjusting U_{s_dc} to be equal to the optimal value, then the equivalent load resistance of secondary side will be adjusted automatically to be equal to R_{l_opt}.

D. PARAMETER SENSITIVITY ANALYSIS

In the process of the maximum efficiency tracking, the value of L_1 may change due to its rising temperature. This will cause errors in mutual inductance estimation. So, a parameter sensitivity analysis about L_1 is necessary. In this section, it is defined that $\rho = L_{real}/L_{ideal}$, where L_{real} is the value of the L_1 when it vary along with the temperature rise, and L_{ideal} is the value which is used to estimate mutual inductance in (14). Then the error of efficiency can be defined as:

$$\delta_\eta = \frac{\eta_{real} - \eta_{ideal}}{\eta_{ideal}} \tag{20}$$

where η_{real} is the efficiency which is calculated by (6), (7) and (14) with L_{real}, η_{ideal} is the efficiency which is calculated by same method with L_{ideal}. The range of ρ is defined from 0.9 to 1.1. The simulated result is shown in Fig.5.

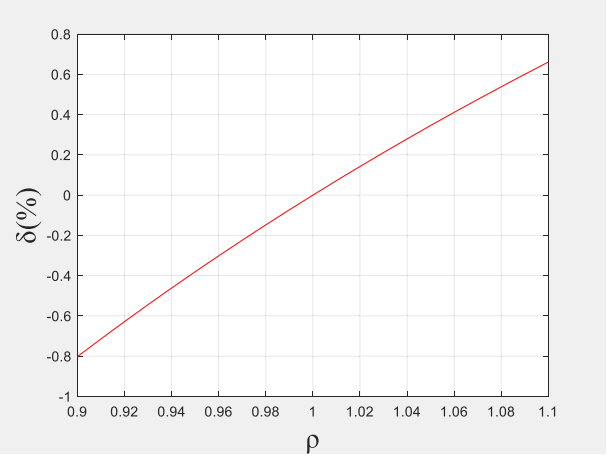

FIGURE 6. Efficiency error δ_η about ρ.

In Fig.5, the abscissa represents ρ, and the ordinate represents δ_η. It can be seen from Fig.6 that when the error of inductance is 10%, the error of efficiency is about 0.8%. The results prove that when the value of inductance changes within reasonable range, the error of efficiency can be ignored. Consequently, the value of L_1 can be assumed as constant in the process of maximum efficiency tracking.

E. PROCESS OF THE MET AND CV CHARGING

The control diagram of WPT system with MET and CV charging method is shown in Fig.7. A PI controller is designed on secondary side to improve the stability of output voltage. In the meantime, the value of R_l and d_2 are transferred to primary side by wireless communication. On the primary side, two steps are necessary to complete the maximum efficiency tracking.

1) Estimate the mutual inductance of the current working status through (14).
2) Calculate the optimal input voltage $U_{s\_dc\_opt}$ of the inverter through (19), and adjust U_{s_dc} to be equal to $U_{s\_dc\_opt}$. The mutual inductance used in (19) is estimated on the previous step. In order to maintain the voltage at a constant level, another PI controller is required for voltage regulation in this process.

The detailed flowchart of the MET and CV charging method is shown in Fig. 8. At first, adjust d_1 to promote U_{s_dc} high enough to drive the secondary side to work stable. Then, the above two steps are carried out in turn at a higher frequency. Through the above methods, the constantly changing mutual inductance and optimal input voltage can be estimated precisely. The maximum efficiency tracking for the dynamic WPT system can be realized by constantly adjusting the input voltage of inverter to be equal to the optimal value.

IV. EXPERIMENTAL STUDIES OF THE PROPOSED MET AND CV CHARGING METHOD

To verify the availability of the proposed method, an experimental platform (shown in Fig.9) is built referring the diagram shown in Fig.7, and the parameters of the system are shown in Table 1. In the WPT system, different DSP chips (TMS320F28335 for primary side, TMS320F28035 for secondary side) are used to design the controllers. Two ZigBee modules are used to establish the wireless communication network to realize data transmission between primary and secondary side. The load is replaced by two 10Ω resistors. One resistor is connected directly to the output port of the system, and another is connected to this port by a switch.

In this experimental platform, a power analyzer, (PW6001, HIOKI) is used to measure the power and efficiency of the system. An oscilloscope, (MDO3054, Tektronix) is used to record the waveform of the voltage and current. A power supply, (62150H-600, Chroma) is used to provide the DC input voltage. An impedance analyzer, (ZGA5920, NF) is used to measure the value of inductance, mutual inductance, capacitance, and internal resistance of the coils.

In the experiment, the MET and CV control method can be verified under the condition of different load and mutual inductance. The change of the load is realized by altering the

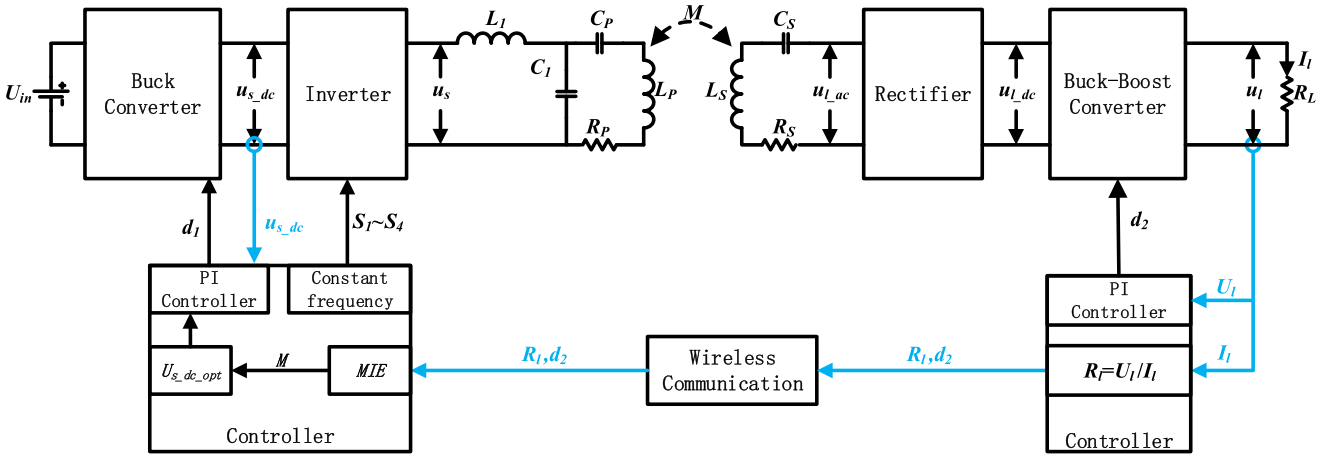

FIGURE 7. Control diagram of WPT system with MET and CV charging.

state of the switch, and the change of the mutual inductance is realized by adjusting the distance of coupling coils.

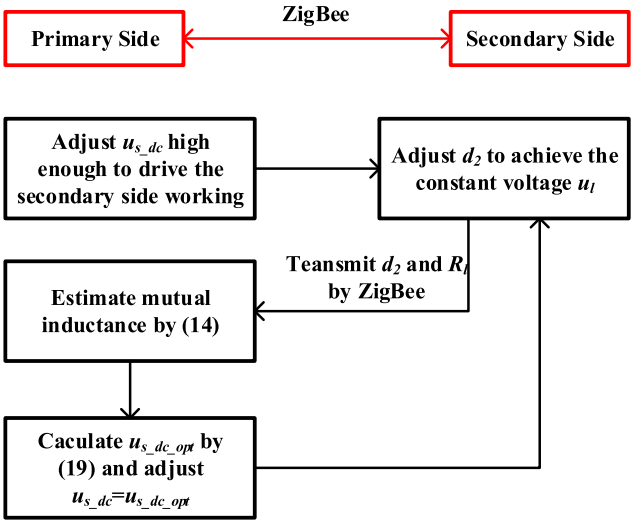

FIGURE 8. Flowchart of the tracking process.

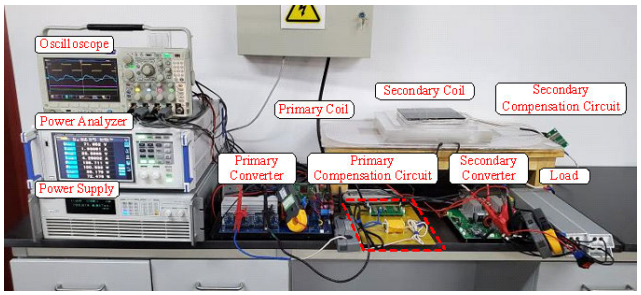

FIGURE 9. Photos of the experiment platform.

A. EXPERIMENT OF THE MIE METHOD

In this section, the experiment is carried out to verify the accuracy of mutual inductance estimation. At a distance from 5 to 20 cm, the comparison between estimated and measured mutual inductance is conducted. The result is shown in Fig.10.

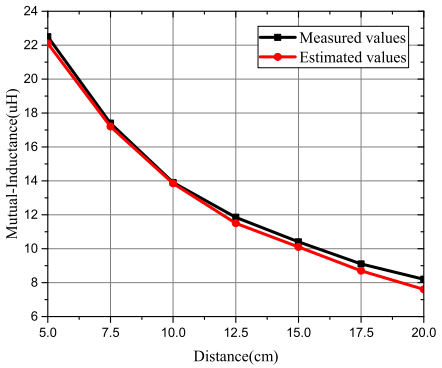

FIGURE 10. Experimental results of mutual inductance estimation.

The abscissa of Fig.10 represents the distance between the coils, and the ordinate represents the value of mutual inductance. In Fig.10, the black line represents the mutual inductance measured by impedance analyzer, and the red line represents the estimated value when $R_l = 5\Omega$. From the results, we can see that the estimated mutual inductance is consistent with the measured value. When the distance of the coils is 6cm, the mutual inductance is about 20μH. When the distance of the coils is 15cm, the mutual inductance is about 10μH. The result shows that the mutual inductance can be estimated accurately by this method.

B. EXPERIMENT OF OPTIMAL INPUT VOLTAGE MATCHING

In this section, the optimal input voltage matching is verified under the condition of different load and mutual inductance. In this experiment, the optimal input voltage $U_{s\_dc\_opt}$ is calculated by MATLAB when $R_l = 10\Omega$ and 5Ω, respectively. And the value of $U_{s\_dc\_opt}$ matched by the platform is also recorded under the same conditions. The experimental results are shown in Fig.11.

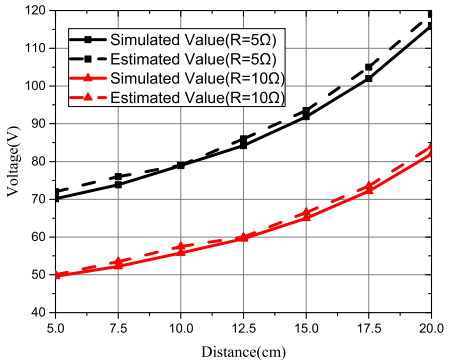

FIGURE 11. Experimental results of optimal voltage matching.

In Fig.11, the abscissa represents the distance between coils, and the ordinate represents the value of optimal input voltage. The black and red solid line indicates the value of $U_{s\_dc\_opt}$ calculated by MATLAB. The black and red dash line indicates that matched by the WPT system. From the result, we can see that the $U_{s\_dc\_opt}$ increases along with the distance. Besides, the value of $U_{s\_dc\_opt}$ estimated by the system is basically consistent with the simulated value. It can be verified that the result of the optimal voltage matching method is in line with our expectation.

C. EXPERIMENT OF MET AND CV CHARGING METHOD

The mutual inductance estimation and optimal input voltage matching are verified in the above experiments. The experiment of MET and CV charging method are carried out in this section. Firstly, the experimental study of the proposed method is conducted under the condition of different resistance. Secondly, the similar study is also carried out under the circumstances of different mutual inductance.

In the first experiment, the mutual inductance remains at 20μH and the resistance is set to 5Ω and 10Ω, respectively. Besides, the progress is also recorded when the resistance is changing from 10Ω to 5Ω. The waveform of the oscilloscope is shown in Fig.12. Channels 1 and 2 are the output voltage and current of the inverter, channels 3 and 4 are the voltage and current of the resistor.

Fig.12(a) and Fig.12(b) show the results when the resistance is 10Ω and 5Ω, respectively. We can see that no matter 10Ω or 5Ω the resistance is, the voltage of the resistor is kept at 24V. The input voltage of the inverter is adjusted to be equal to 54V and 74V, respectively. The results are matched with Fig.11. Due to the load is not heavy, the output current of inverter has a little distortion which is in the reasonable range. From Fig.12(c), it can be seen in the process of resistance changing from 10Ω to 5Ω that the output voltage remains stable at 24V while the input voltage rises from 54V to 74V in 50ms to realizing maximum efficiency tracking.

In the above experiments, it can be verified that the proposed MET and CV charging method is well adapted for the condition that the resistance changes suddenly. In fact, the equivalent load of movable devices does not change

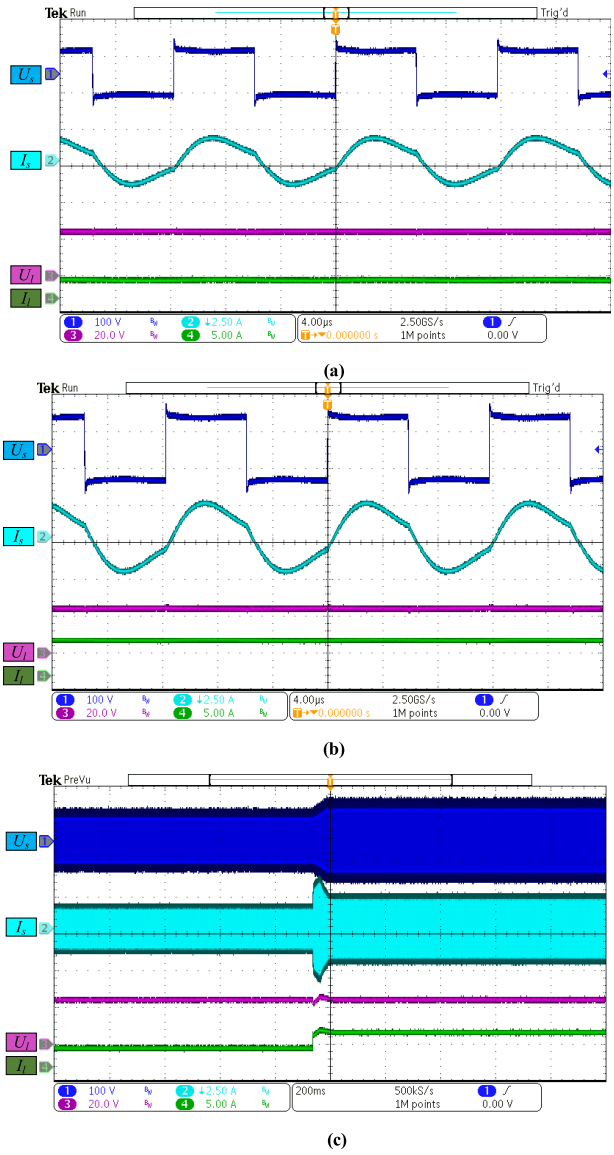

FIGURE 12. The output voltage and current of inverter and load when M=20μH. (a) The resistance is 10Ω. (b) The resistance is 5Ω. (c) The resistance is turned from 10Ω to 5Ω.

rapidly. The process of change is slower than that in the experiment.

In the second experiment, the resistance is constant at 5Ω, and the distance between the coils are gradually increased from 6cm to 15cm. In this range, the mutual inductance changes between 10 and 20μH. The waveform of the oscilloscope is also recorded in Fig.13.

Fig.13(a) shows the waveforms when the resistance is 5Ω and the mutual inductance is about 10μH. Compared with Fig.12(b), it can be found that the voltage of the resistor is kept at 24V regardless of mutual inductance is 10μH or 20μH. The input voltage of the inverter is adjusted to be equal to 74V and 92V, respectively. It also matches with Fig.11. In Fig.13(b), it can be found that the input voltage

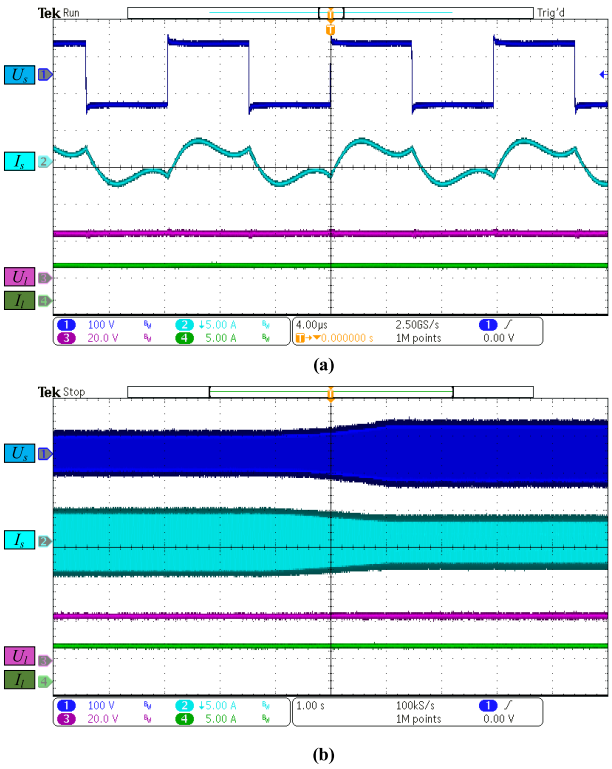

FIGURE 13. The output voltage and current of inverter and load when $R_l = 5\Omega$. (a) M=10μH. (b) M is changed from 20μH to10μH.

increases along with the distance of the coils, and the voltage of the resistor remains at 24V.

From all above experiments, it can be verified that the MET and CV charging method proposed in this paper is perfectly in line with our expectations. Whether the mutual inductance or resistance changes, the input voltage of inverter is always adjusted to be equal to the optimal value by the proposed control method accurately.

D. ANALYSIS OF EFFICIENCY

In the above experiments, the proposed MET and CV charging method are verified. In this section, the efficiency of the system is compared through the following experiments. Firstly, the comparative study is conducted under the conditions whether the proposed MET method is applied. Secondly, the efficiency of the system is compared under the conditions of different mutual inductance and resistance. The results are shown in Fig.14.

Fig.14(a) is the screenshot of the PW6001 when the system works at the condition that $M = 20\mu$H and $R_l = 5\Omega$. Fig.14(b) shows the efficiency whether the MET method is applied or not. The red line represents the efficiency with MET control method is not applied. The black line represents that when the MET control method is adopted. In Fig.14(c), the curve of efficiency is plotted with the change of mutual inductance. The black and red solid line represent the efficiency simulated by MATLAB under the condition of R_l is

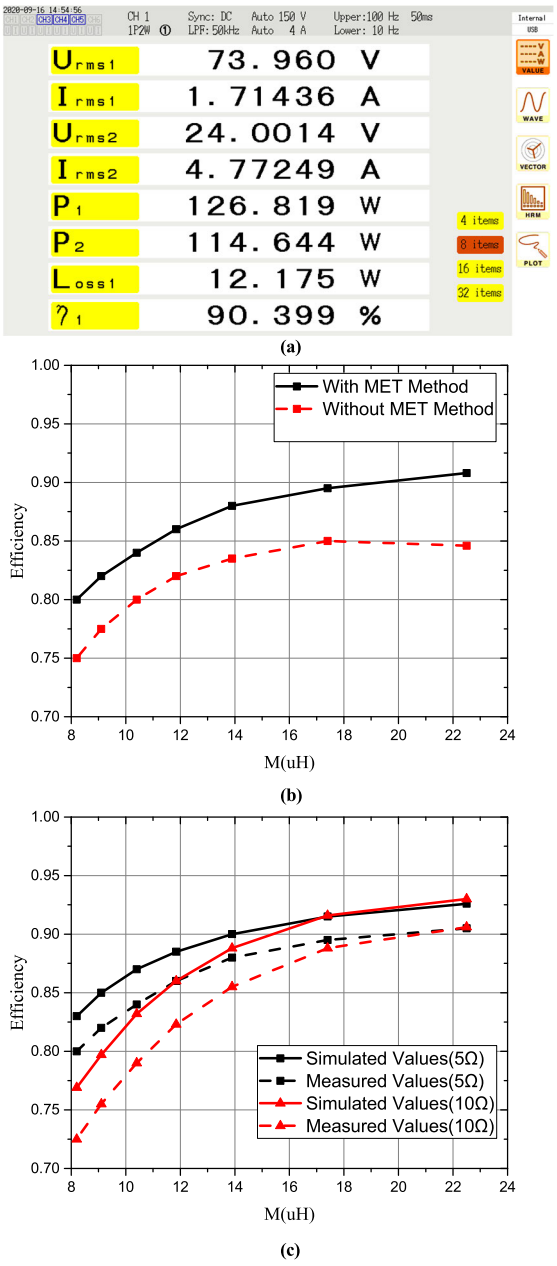

FIGURE 14. Analysis of the system efficiency. (a) Photo of efficiency measured by PW6001. (b) Efficiency whether the MET method is applied or not. (c) Efficiency under different resistances and mutual inductance.

5Ω and 10Ω, respectively. And the black and red dash line represent the efficiency measured by PW6001.

It can be seen from the Fig.14(b) that the efficiency of the system in which the MET method is not adopted is always lower than that adopts MET method. This indicates that the proposed method can improve the efficiency of the system.

Besides, it can be found from Fig.14(c) that the measured efficiency is consistent with the simulated results. But the measured efficiency is always lower than simulation value especially in the case of low mutual inductance. Because in the process of analysis, we do not consider the loss of

TABLE 2. Comparison with previous method.

Reference	Control Principle	Speed	Maximum Efficiency	Wireless Communication	Dynamic WPT system	Wide Load	Soft Switch	CV/CC
This paper	Optimal Input Voltage Matching	Excellent	88%	YES	YES	Excellent	YES	YES
[17]@2020	Minimum Input Current Searching	General	86%	NO	NO	General	NO	YES
[18]@2018	Minimum Input Current Searching	General	65%	NO	NO	Excellent	NO	YES
[19]@2018	Optimal Load Resistance Matching	Good	85%	YES	NO	Excellent	YES	YES
[20]@2018	ON-OFF Switch Mode	General	72.6%	YES	NO	General	YES	NO
[21]@2018	Pulse Density Modulation	General	85%	NO	NO	General	YES	NO

MOSFETs. For the LCC resonant topology, the MOSFETs are working in ZVS condition. That means the switching loss is greatly reduced. Besides, the reason why the error increases when the mutual inductance is small is that the impedance of the coils is detuned. This greatly reduces the accuracy of the proposed method. It should be noted that the phenomenon is universal in the previous research results.

To summarize, it is feasible that the proposed method in this paper can accurately realize the maximum efficiency tracking and constant output voltage.

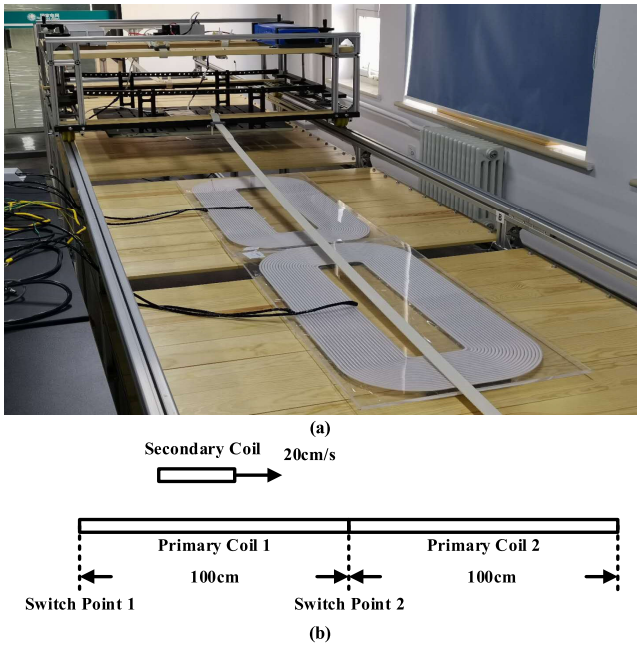

FIGURE 15. The photo and diagram of dynamic WPT experiment. (a) The photo of dynamic WPT platform. (b) The sketch of dynamic WPT experiment.

E. EXPERIMENT OF DYNAMIC WPT SYSTEM

In order to verify the feasibility of the proposed MET and CV charging method for dynamic WPT system, a new experiment is carried out. The photo of dynamic WPT experimental platform is shown in Fig.15(a) and the sketch of the dynamic experiment is shown in Fig.15(b). In this experiment, the distance of the coils is kept at 6cm, and the secondary side moves above the primary coils at the speed of 20cm/s. The inverter is connected to the primary coil 1 and coil 2 when the center of secondary coil meets point 1 and point 2, respectively. The parameters and appearance of primary coils is kept consistent. However, if cutting off the connection between the inverter and the resonant circuit when the system is running, it will cause transient overvoltage in the inductance. Therefore, about 50ms is reserved for the inverter to switch from coil 1 to coil 2. In the reserved time, the input voltage of the inverter drops to 0V. In the whole experiment, the waveform of the oscilloscope is recorded in Fig.16.

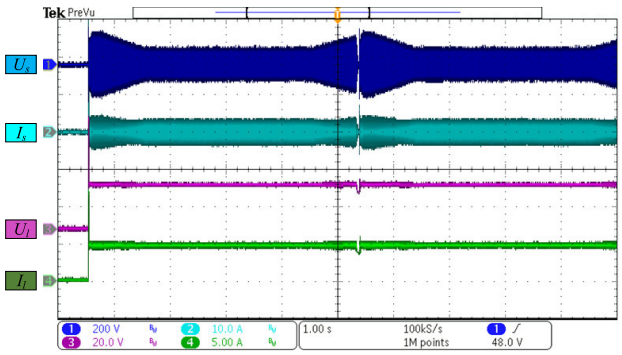

FIGURE 16. The waveform of dynamic WPT experiment.

It can be seen from Fig.16 that U_s is adjusted to about 150V after the primary coil 1 is connected to the inverter and the output voltage is maintained at 24V immediately. Then, with the secondary side moving, U_s decreases from 150V to 74V. Because the mutual inductance between the coils increases gradually in this area. In the following time, U_s is maintained at about 74V. In this area, the mutual inductance remains constant. Before the secondary side leaves the primary coil 1, U_s increases gradually because the mutual inductance decreases. In the whole period, the output voltage is maintained at 24V, and U_s is matched to the optimal value by the proposed MET and CV charging methods. In the above experiments, the proposed method is applied in dynamic WPT system perfectly.

F. COMPARISON WITH PREVIOUS METHODS

In recent years, different methods for constant current/voltage charging and maximum efficiency tracking have been reported. In order to show the difference between these methods, a fair comparison is carried out. In this comparison, the factors considered include the control principle, speed, maximum efficiency, the wireless communication, static or dynamic WPT system, wide load, soft switch condition and CV/CC charging condition. The result is shown in Table 2. It should be noted that the efficiency measured in the above experiments does not consider the losses of the buck converter in the primary side, the actual maximum efficiency is about 88% under the whole WPT system.

V. CONCLUSION

In this paper, a maximum efficiency tracking and constant voltage charging method is proposed for dynamic WPT system with LCC-S resonant topology. Compared with existing methods, this method can quickly estimate the dynamic mutual inductance and match the optimal input voltage in a certain frequency. The effectiveness of this method is proved by mathematical derivation and experiment, respectively. The final experiment shows that this method cannot only improve the stability of the output voltage, but also always track the maximum efficiency point no matter the mutual inductance and equivalent load changes. It is very suitable for dynamic WPT system. However, the accuracy of maximum efficiency tracking is bad in the case of low coupling coefficient. It is because that the system is not in the ideal resonance state. It is also the common problem of the existing methods. In addition, this paper focuses on the maximum efficiency tracking of the secondary side above a single primary coil, it didn't consider the effect between the primary adjacent coils. This is also a problem to be solved in future. The MET method proposed in this paper is applied to the dynamic WPT system of movable inspection robot. The speed of it is smaller than other devices like EV. The accuracy of MET will decrease because of the delay of wireless communication. In general, when there is a 2cm misalignment between the coils, the error of estimated mutual inductance is not large. If considering the 2ms delay of wireless communication, the speed of the device can reach 10m/s. Although the speed is still smaller than that of EV, it is also acceptable to most dynamic WPT systems.

REFERENCES

[1] K. Song, Z. Li, J. Jiang, and C. Zhu, "Constant current/voltage charging operation for series–series and series–parallel compensated wireless power transfer systems employing primary-side controller," *IEEE Trans. Power Electron.*, vol. 33, no. 9, pp. 8065–8080, Sep. 2018, doi: 10.1109/TPEL.2017.2767099.

[2] T. Fujita, T. Yasuda, and H. Akagi, "A dynamic wireless power transfer system applicable to a stationary system," *IEEE Trans. Ind. Appl.*, vol. 53, no. 4, pp. 3748–3757, Jul. 2017, doi: 10.1109/TIA.2017.2680400.

[3] M. Su, Z. Liu, Q. Zhu, and A. P. Hu, "Study of maximum power delivery to movable device in omnidirectional wireless power transfer system," *IEEE Access*, vol. 6, pp. 76153–76164, 2018, doi: 10.1109/ACCESS.2018.2883503.

[4] R. Mai, Y. Liu, Y. Li, P. Yue, G. Cao, and Z. He, "An active-rectifier-based maximum efficiency tracking method using an additional measurement coil for wireless power transfer," *IEEE Trans. Power Electron.*, vol. 33, no. 1, pp. 716–728, Jan. 2018, doi: 10.1109/TPEL.2017.2665040.

[5] M. R. Basar, M. Y. Ahmad, J. Cho, and F. Ibrahim, "An improved wearable resonant wireless power transfer system for biomedical capsule endoscope," *IEEE Trans. Ind. Electron.*, vol. 65, no. 10, pp. 7772–7781, Oct. 2018, doi: 10.1109/TIE.2018.2801781.

[6] A. Zakerian, S. Vaez-Zadeh, and A. Babaki, "A dynamic WPT system with high efficiency and high power factor for electric vehicles," *IEEE Trans. Power Electron.*, vol. 35, no. 7, pp. 6732–6740, Jul. 2020, doi: 10.1109/TPEL.2019.2957294.

[7] Y. Jiang, L. Wang, J. Fang, C. Zhao, K. Wang, and Y. Wang, "A joint control with variable ZVS angles for dynamic efficiency optimization in wireless power transfer system," *IEEE Trans. Power Electron.*, vol. 35, no. 10, pp. 11064–11081, Oct. 2020, doi: 10.1109/TPEL.2020.2977849.

[8] M. Zhang, L. Tan, J. Li, and X. Huang, "The charging control and efficiency optimization strategy for WPT system based on secondary side controllable rectifier," *IEEE Access*, vol. 8, pp. 127993–128004, 2020, doi: 10.1109/ACCESS.2020.3007444.

[9] S. Ruddell, U. K. Madawala, and D. J. Thrimawithana, "Dynamic WPT system for EV charging with integrated energy storage," *IET Power Electron.*, vol. 12, no. 10, pp. 2660–2668, Aug. 2019, doi: 10.1049/iet-pel.2018.5848.

[10] Y. Chen, H. Zhang, S.-J. Park, and D.-H. Kim, "A switching hybrid LCC-S compensation topology for constant current/voltage EV wireless charging," *IEEE Access*, vol. 7, pp. 133924–133935, 2019, doi: 10.1109/ACCESS.2019.2941652.

[11] T. C. Beh, M. Kato, T. Imura, S. Oh, and Y. Hori, "Automated impedance matching system for robust wireless power transfer via magnetic resonance coupling," *IEEE Trans. Ind. Electron.*, vol. 60, no. 9, pp. 3689–3698, Sep. 2013, doi: 10.1109/TIE.2012.2206337.

[12] S. Jeong, T.-H. Lin, and M. M. Tentzeris, "Range-adaptive impedance matching of wireless power transfer system using a machine learning strategy based on neural networks," in *IEEE MTT-S Int. Microw. Symp. Dig.*, Boston, MA, USA, Jun. 2019, pp. 1423–1425, doi: 10.1109/MWSYM.2019.8700996.

[13] Y. Liu and H. Feng, "Maximum efficiency tracking control method for WPT system based on dynamic coupling coefficient identification and impedance matching network," *IEEE J. Emerg. Sel. Topics Power Electron.*, vol. 8, no. 4, pp. 3633–3643, Dec. 2020, doi: 10.1109/JESTPE.2019.2935219.

[14] Y. Li, W. Dong, Q. Yang, J. Zhao, L. Liu, and S. Feng, "An automatic impedance matching method based on the feedforward-backpropagation neural network for a WPT system," *IEEE Trans. Ind. Electron.*, vol. 66, no. 5, pp. 3963–3972, May 2019, doi: 10.1109/TIE.2018.2835410.

[15] H. Li, J. Li, K. Wang, W. Chen, and X. Yang, "A maximum efficiency point tracking control scheme for wireless power transfer systems using magnetic resonant coupling," *IEEE Trans. Power Electron.*, vol. 30, no. 7, pp. 3998–4008, Jul. 2015, doi: 10.1109/TPEL.2014.2349534.

[16] K. Song, R. Wei, G. Yang, H. Zhang, Z. Li, X. Huang, J. Jiang, C. Zhu, and Z. Du, "Constant current charging and maximum system efficiency tracking for wireless charging systems employing dual-side control," *IEEE Trans. Ind. Appl.*, vol. 56, no. 1, pp. 622–634, Jan. 2020, doi: 10.1109/TIA.2019.2942278.

[17] Y. Yang, W. Zhong, S. Kiratipongvoot, S.-C. Tan, and S. Y. R. Hui, "Dynamic improvement of series–series compensated wireless power transfer systems using discrete sliding mode control," *IEEE Trans. Power Electron.*, vol. 33, no. 7, pp. 6351–6360, Jul. 2018, doi: 10.1109/TPEL.2017.2747139.

[18] X. Dai, X. Li, Y. Li, and A. P. Hu, "Maximum efficiency tracking for wireless power transfer systems with dynamic coupling coefficient estimation," *IEEE Trans. Power Electron.*, vol. 33, no. 6, pp. 5005–5015, Jun. 2018, doi: 10.1109/TPEL.2017.2729083.

[19] W. Zhong and S. Y. R. Hui, "Maximum energy efficiency operation of series-series resonant wireless power transfer systems using on-off keying modulation," *IEEE Trans. Power Electron.*, vol. 33, no. 4, pp. 3595–3603, Apr. 2018, doi: 10.1109/TPEL.2017.2709341.

[20] H. Li, J. Fang, S. Chen, K. Wang, and Y. Tang, "Pulse density modulation for maximum efficiency point tracking of wireless power transfer systems," *IEEE Trans. Power Electron.*, vol. 33, no. 6, pp. 5492–5501, Jun. 2018, doi: 10.1109/TPEL.2017.2737883.

[21] W. Li, H. Zhao, J. Deng, S. Li, and C. C. Mi, "Comparison study on SS and double-sided LCC compensation topologies for EV/PHEV wireless chargers," *IEEE Trans. Veh. Technol.*, vol. 65, no. 6, pp. 4429–4439, Jun. 2016, doi: 10.1109/TVT.2015.2479938.
[22] H. Feng, T. Cai, S. Duan, J. Zhao, X. Zhang, and C. Chen, "An LCC-compensated resonant converter optimized for robust reaction to large coupling variation in dynamic wireless power transfer," *IEEE Trans. Ind. Electron.*, vol. 63, no. 10, pp. 6591–6601, Oct. 2016, doi: 10.1109/TIE.2016.2589922.
[23] V.-B. Vu, D.-H. Tran, and W. Choi, "Implementation of the constant current and constant voltage charge of inductive power transfer systems with the double-sided LCC compensation topology for electric vehicle battery charge applications," *IEEE Trans. Power Electron.*, vol. 33, no. 9, pp. 7398–7410, Sep. 2018, doi: 10.1109/TPEL.2017.2766605.
[24] J. Qi, "Analysis, design, and optimisation of an LCC/S compensated WPT system featured with wide operation range," *IET Power Electron.*, vol. 13, no. 9, pp. 1819–1827, Jul. 2020, doi: 10.1049/iet-pel.2019.1305.
[25] X. Hu, Y. Wang, Y. Jiang, W. Lei, and X. Dong, "Maximum efficiency tracking for dynamic wireless power transfer system using LCC compensation topology," in *Proc. IEEE Energy Convers. Congr. Expo. (ECCE)*, Portland, OR, USA, Sep. 2018, pp. 1992–1996, doi: 10.1109/ECCE.2018.8557494.

HAO HE was born in Jining, Shandong, China. He received the B.S. and M.S. degrees in control engineering from Tiangong University, Tianjin, China, in 2014 and 2017, respectively. He is currently pursuing the Ph.D. degree in electrical engineering with the China Electric Power Research Institute, Beijing, China. His research interests include wireless power transfer and power electronics.

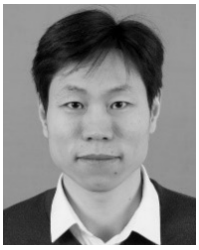

SONGCEN WANG was born in Henan, China, in 1979. He received the B.S. degree in control theory and control engineering from North China Electric Power University, Beijing, China, in 2001, and the M.S. and Ph.D. degrees in power electronics from the China Electric Power Research Institute (CEPRI), in 2004 and 2010, respectively. From November 2014 to October 2015, he was an Academic Visitor with Aalborg University, Denmark. He is currently working as a Senior Engineer with the Department of Electrical Engineering, CEPRI. His current research interests include wireless power transfer and power electronics.

YOUWEI LIU received the B.Sc. and M.Sc. degrees in electrical engineering from Xi'an Jiaotong University, Xi'an, China, in 1983 and 1986, respectively, and the Ph.D. degree from the China Electric Power Research Institute (CEPRI), Beijing, China, in 1992. Since 2003, he has been a Professor with CEPRI. His research interests include high-voltage insulation, monitoring and diagnosis of high-voltage equipment, and smart substation.

CHENG JIANG was born in Nanchong, Sichuan, China. He received the B.E. degree in automation and the Ph.D. degree in control theory and control engineering from the College of Automation, Chongqing University, Chongqing, China, in 2013 and 2019, respectively. He is currently working with the China Electric Power Research Institute, Beijing, China. His research interests include wireless power transfer and power electronics.

XIAOKANG WU was born in Zhoukou, Henan, China. He received the B.S. and M.S. degrees in electrical engineering and control engineering from Tiangong University, Tianjin, China, in 2014 and 2017, respectively. Since 2017, he has been working with the China Electric Power Research Institute (CEPRI). His research interest includes wireless power transfer.

BIN WEI was born in Hubei, China, in 1978. He received the B.S. degree in power system and automation from the Changsha University of Science and Technology, in 2002, and the Ph.D. degree in engineering (applied superconductivity) from the Huazhong University of Science and Technology, in 2007. Since 2007, he has been working with the China Electric Power Research Institute (CEPRI). His research interests include applied superconductivity and wireless power transfer.

BINGWEI JIANG was born in Yancheng, Jiangsu, China. He received the B.S. degree in electric engineering from the Yancheng Institute of Technology, Yancheng, in 2019. He is currently pursuing the M.S. degree in electrical engineering with the China Electric Power Research Institute, Beijing, China. His research interest includes wireless power transfer.